

Original Research Article

Soil Moisture Modelling using Remote Sensing and Artificial Neural Networks: A Study of Devbhumi Dwarka Region

ABSTRACT

For the arid and semi-arid region of Devbhumi Dwarka in Gujarat, where soil moisture issue is prominent, a GIS-based approach is needed to develop models for estimation of soil moisture. In this study, Landsat and Sentinel data were used to develop multiple soil moisture indices. Using these spectral indices, artificial neural network (ANN) models were developed using actual recorded soil moisture data. Total of 174 samples were collected in the study area of 3,77,731 ha. Values of soil moisture ranged from 3.40 % to 12.50 % with an average value of 8.42 %. The maps of soil moisture indices i.e. LST, NDVI, NDWI, NSDSI3, MI and VSWI were generated on 1:550000 scale using ArcMap software. Moisture index NSDSI3 was highest correlating index. Best ANN model for soil moisture content (SMC) estimation was developed using Sentinel data (8-14-1) with RMSE, R^2 and NRMSE values of 0.85 %, 0.73 and 0.10 for training and 1.11 %, 0.54 and 0.13 for testing respectively.

Key words: *Soil moisture modelling, Remote Sensing, GIS, ANN, Spectral indices*

1. INTRODUCTION

Soil, a finite and non-renewable natural resource, plays a critical role in sustaining agricultural productivity. In India, the per capita availability of land has dwindled due to population escalation, emphasizing the need for effective land and water management practices to enhance crop production. The focus of this paper is on the critical aspect of soil moisture estimation through remote sensing and GIS in Devbhumi Dwarka region, emphasizing its significance for sustainable land and water management practices.

The estimation of soil moisture is a complex yet essential task for understanding and optimizing agricultural processes. Various methods, including gravimetric techniques, moisture sensors and remote sensing technologies, have been employed to measure or estimate soil moisture. Ground-based techniques, such as gravimetric methods and soil moisture sensors, offer precise data for specific point locations but are limited by labour intensity and spatial coverage. In contrast, remote sensing techniques, utilizing platforms like Landsat and Sentinel, provide a cost-effective and efficient means to monitor soil moisture over large spatial areas, overcoming the challenges posed by traditional ground-based sampling networks.

Recent advancements in remote sensing, particularly with platforms like Sentinel-2 and Landsat-8, have revolutionized soil moisture assessment. These satellites, equipped with moderate-resolution sensors, offer valuable data for large-scale dynamic monitoring. This paper explores the practical utility of remote sensing techniques in mapping and modelling soil moisture, providing a comprehensive understanding of its spatial-temporal variations.

Soil moisture, crucial for optimal crop water productivity, demands accurate determination. Ex-situ methods like the gravimetric method, though accurate, are labour-intensive (Reynolds, 1970). Garg *et al.* (2016) highlighted the efficacy of sensors like GMS,

TDR, and FDR, emphasizing cost-effectiveness and accuracy in varying soil types. In-situ methods, including FDR and TDR, present viable options with high correlation coefficients.

Sharma *et al.* (2018) conducted a comprehensive review of soil moisture estimation methods, differentiating point measurements and remote sensing. They concluded that while TDR provides accurate results with minimal soil disturbance, remote sensing offers broader coverage but requires initial ground truthing. Similarly, Gojiya *et al.* (2023a) have reviewed comprehensively various soil moisture measurement and estimation methods with efficiency of GIS based moisture estimation. Liu *et al.* (2021) delved into the application of Sentinel-2 bands for soil moisture estimation, providing valuable insights into the spatial distribution of soil moisture at different depths.

Hassan-Esfahani *et al.* (2015) leveraged artificial neural network (ANN) models with spectral images to estimate surface soil moisture, demonstrating impressive accuracy. Khanmohammadi *et al.* (2015) explored NDVI, NDMI, and LST indices for surface soil moisture estimation, showcasing a reasonable correlation. Welikhe *et al.* (2017) utilized MSI to estimate soil moisture in Alabama, establishing its efficiency in areas lacking in-situ data. Liu *et al.* (2021) compared different indices for soil moisture estimation, highlighting the effectiveness of MI under various land cover types. Rabie *et al.* (2021) employed Sentinel-1 radar and Sentinel-2 multispectral imagery with machine learning algorithms for surface soil moisture estimation, showcasing high accuracy. Sedaghat *et al.* (2022) employed spectral indices, RF, and MLR for surface soil moisture estimation, highlighting the superiority of the RF method. Sharma *et al.* (2022) examined trends in NDVI and its correlation with LST, SM, and precipitation, emphasizing NDVI's sensitivity to LST. Gojiya *et al.* (2023b) reviewed multiple studies modelling soil properties such as soil salinity and soil moisture. Dubayah *et al.* (2023) explored multiscale properties of soil moisture fields using passive microwave sensing and distributed models, underlining the success of passive microwave remote sensing in soil moisture determination. The review literature emphasizes the critical role of soil moisture in plant growth and crop water productivity. It compares ex-situ methods like gravimetric and calcium carbide with in-situ methods including FDR, TDR, and capacitance-based sensors. Additionally, remote sensing and GIS techniques, such as Sentinel-2 bands and artificial neural networks, are explored for soil moisture estimation, highlighting their effectiveness in diverse conditions.

Various studies have been done on modelling soil moisture using GIS techniques. As these models are area specific, these models need to be developed for the area of interest. Soil moisture modelling is of utmost importance for arid and semi-arid area like Devbhumi Dwarka. In the present study, soil moisture measurements were obtained through the gravimetric method. Subsequently, Artificial Neural Network (ANN) models were constructed utilizing these measurements, employing Landsat and Sentinel datasets, specifically focusing on the Devbhumi Dwarka region in Gujarat, India.

1.1 Study Area Overview

The research focused on the coastal belt of Devbhumi Dwarka district, Gujarat, India, situated on the southern coast of the Gulf of Kutch. The district comprises four talukas, spanning latitudes 21.89° N to 22.31° N and longitudes 69.33° E to 69.71° E. The study specifically aimed at the coastal talukas of Dwarka, Khambhalia, and Kalyanpur, collectively covering 3,77,731 ha (Fig. 1).

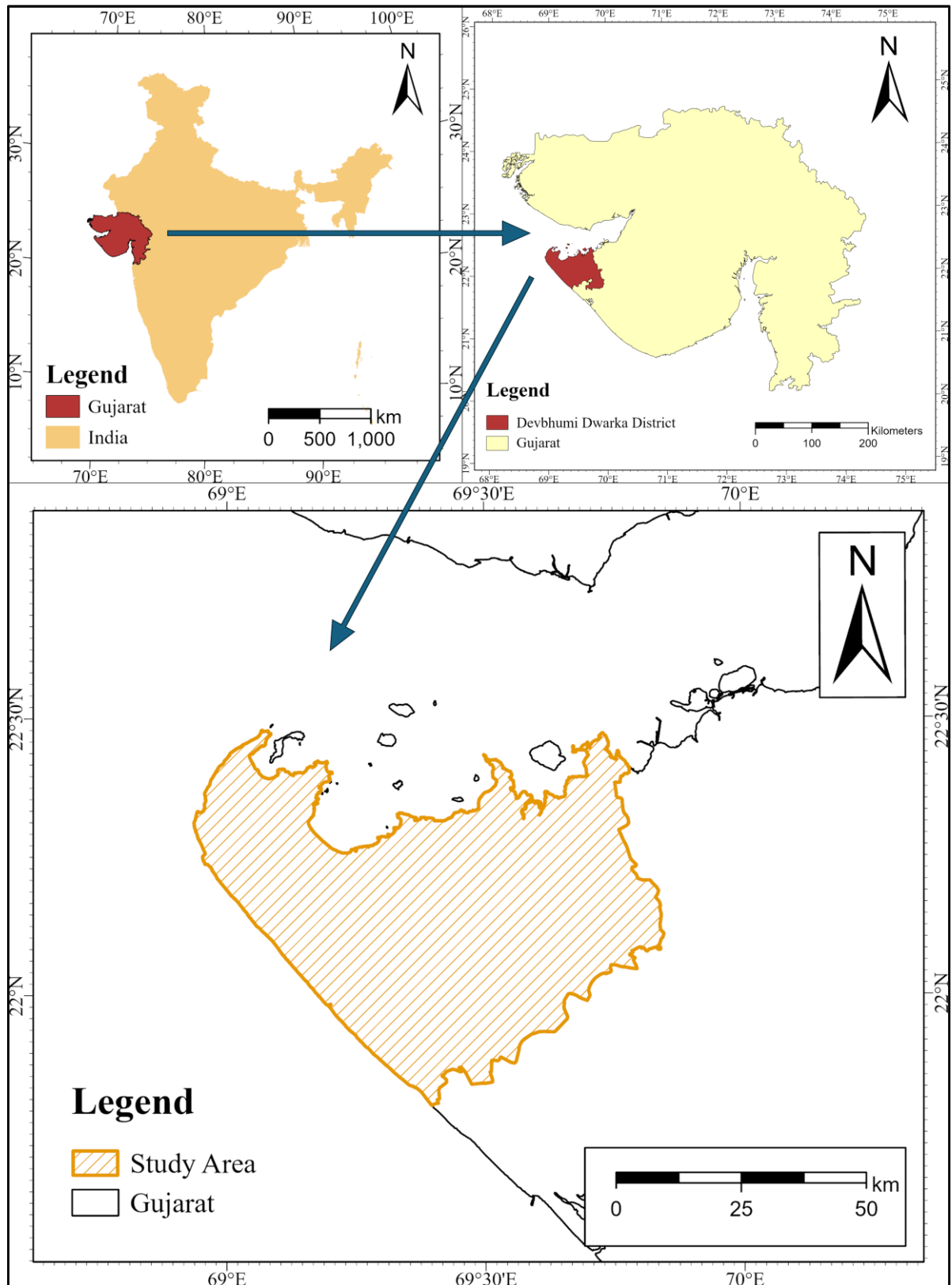


Fig. : Location of the study area

The climate of the study area is characterized as semi-arid (BS_h) according to the Koppen and Geiger classification. This climate type is associated with hot, often extremely hot, summers and mild to cool winters, featuring minimal precipitation. Devbhumi Dwarka

district experiences an average annual highest temperature of 36.9 °C, an average annual lowest temperature of 14.9 °C, and an annual rainfall of 640 mm (1990-2019). The district's major crops include groundnut, cotton, cumin, gram, coriander, sesame, wheat, garlic, and onion (Anon., 2022b; GSDMA, 2022).

2. METHODOLOGY

2.1 Satellite datasets

The soil moisture samples were taken in non-cloudy in second week of November from 9th to 11th November, 2022. Soil sampling was planned on the satellite visit days consequently. Total three Landsat tiles were necessary to cover the entire study area, while two of Sentinel tiles were combined to cover the study area. The details of satellite images used in the study are given in Table 1. Landsat data included surface reflectance as well as surface temperature data while sentinel data only comprised of surface reflectance.

Table 1: Details of satellite images used

Spacecraft	Dataset Name			
	Processing Level	Sensor ID	Tiling Grid	Date Acquired
Landsat 8	Level 2	OLI-TIRS	WRS 150-045	11-11-2022
Landsat 9	Level 2	OLI-TIRS	WRS 151-044	09-11-2022
Landsat 9	Level 2	OLI-TIRS	WRS 151-045	09-11-2022
Sentinel-2B	Level 2A	MSI	UTM 42QVK	11-11-2022
Sentinel-2B	Level 2A	MSI	UTM 42QWK	11-11-2022

2.2 Field Data Collection

Utilizing a Random within Grid sampling method, 174 soil samples were systematically collected across the area with a 5 × 5 km grid overlaying the study area, each grid containing at least one sample. The soil sampling is shown in Fig. 2. The strategy, designed for representativity and accessibility, involved GPS recording and real-time tracking using the Google Earth app. Some grids, especially near salt farms near sea bay, remained inaccessible. Soil samples, 5 cm deep, were collected in air-tight plastic lock bags.



Fig. 2: Soil sampling at different sites

2.3 Measurement of Soil Moisture Content

The gravimetric method, involving drying soil at 105 °C for 24 hours, was used to determine soil moisture content (SMC). The moisture content in dry weight basis was calculated using following formula. (Reynolds, 1970).

$$\text{Soil Moisture (\%)} = \left(\frac{\text{weight of wet soil} - \text{weight of dry soil}}{\text{weight of dry soil}} \right) \times 100$$

Fig. 3 shows the soil moisture content measuring process.



Fig. 3: Measurement of soil moisture content (SMC)

2.4 Satellite Data Pre-processing

Acquired images were at Level 2 processing, meeting high-quality standards as Analysis Ready Data (CARD)-compliant, endorsed by CEOS. This involves generating Surface Reflectance (SR) and Surface Temperature (ST), ensuring consistent radiance measurements and facilitating change detection.

2.5 Rescaling for Data Utilization

To use Level 2 surface reflectance and temperature data, a rescaling process was applied using specific factors for Landsat and Sentinel datasets. This ensures accurate and comparable utilization of the data.

For Landsat surface reflectance products, the following rescaling equation was applied:

$$\text{Surface reflectance} = (\text{Data} \times 0.0000275) + (-0.2)$$

For Sentinel surface reflectance products, the following rescaling equation was applied:

$$\text{Surface reflectance} = (\text{Data} \times 0.0000275) + (-0.2)$$

For Landsat surface temperature products, the following rescaling equation was applied:

$$\text{Land Surface temperature} = (\text{Data} \times 0.00341802) + 149.0$$

This rescaled surface temperature represents the temperature of the Earth's surface in Kelvin (K) which can be converted to degree centigrade (°C) using raster calculator easily.

These adjustments using raster calculator tools in ArcMap were crucial for accurate interpretation and comparison of the satellite data.

2.6 Soil moisture indices

The following soil moisture indices were developed using the satellite data.

2.6.1 Normalised Difference Vegetation Index (NDVI)

NDVI (Rouse *et al.*, 1974) was computed as an index of plant “greenness” and it attempts to track photosynthetic activity. NDVI values range from -1 to +1, where higher positive values indicate the presence of greener and healthier plants.

$$NDVI = \frac{NIR - R}{NIR + R}$$

Where, NIR = Reflectance in near-infrared band
R = Reflectance in the red visible band

2.6.2 Normalized Difference Water Index (NDWI)

NDWI is a ratio between the NIR and SWIR values. NDWI was calculated using the following formula (Gao, 1996):

$$NDWI = \frac{NIR - SWIR}{NIR + SWIR}$$

The value of NDWI ranges from -1 to +1. NDWI is sensitive to changes in soil moisture which are strongly related to vegetation drought conditions. The average NDWI remains consistently lower than 0.3 under drought conditions and higher than 0.4 under non-drought conditions. This index is also known as Land Surface Water Index (LSWI) and Normalised Difference Moisture Index (NDMI) (EOS Data Analytics, 2022).

2.6.3 Normalized Shortwave-Infrared Difference Soil Moisture Index (NSDSI3)

Remote sensing-based observations of bare soil moisture from broadband remote sensing are of great value as they provide both high temporal and spatial resolution soil moisture in local areas. This index was proposed by Yue *et al.* (2019), using different water absorption in shortwave-infrared bands. Four traditional hyperspectral-based bare-soil moisture indices were used to develop this index.

$$NSDSI3 = \left(\frac{SWIR1 - SWIR2}{SWIR1 + SWIR2} \right)$$

2.6.4 Moisture Index (MI)

Moisture index was calculated by using following formula (Rohde and Olson, 1970). This multispectral index has been proposed for use in describing surface moisture characteristics.

$$MI = \frac{NIR}{B}$$

2.6.5 Vegetation Supply Water Index (VSWI)

The VSWI assumes that under normal conditions, with sufficient soil water supply, land surface temperature observed over vegetation have low values due to cooling effects of evapotranspiration. Vegetation Supply Water Index (VSWI) is the ratio of NDVI to LST (Carlson *et al.*, 1995) as given below.

$$VSWI = \frac{NDVI}{LST}$$

2.7 Modelling SMC using Artificial Neural Network (ANN)

All spectral indices for soil moisture content were used as input data to the artificial neural network and soil parameters i.e., soil moisture was output data to train ANN model. To further eliminate inputs, higher correlation inputs were chosen, and inputs were removed until best input combination was achieved as suggested by Wang *et al.* (2021).

The most important attribute of a layered neural network design is choosing the architecture. Various training algorithms are available like Levenberg Marquardt, Bayesian Regulation, Conjugate Gradient Descent, etc. Levenberg Marquardt is found to be superior by many researchers in various soil properties modelling (Hassan-Esfahani *et al.*, 2015; Alexakis *et al.*, 2017; Wang *et al.*, 2021), which mostly outperforms other algorithms. Feed forward backpropagation neural network with Levenberg Marquardt algorithm was chosen in the study. Overall process flow of the work carried out is shown in flow diagram in Fig. 4.

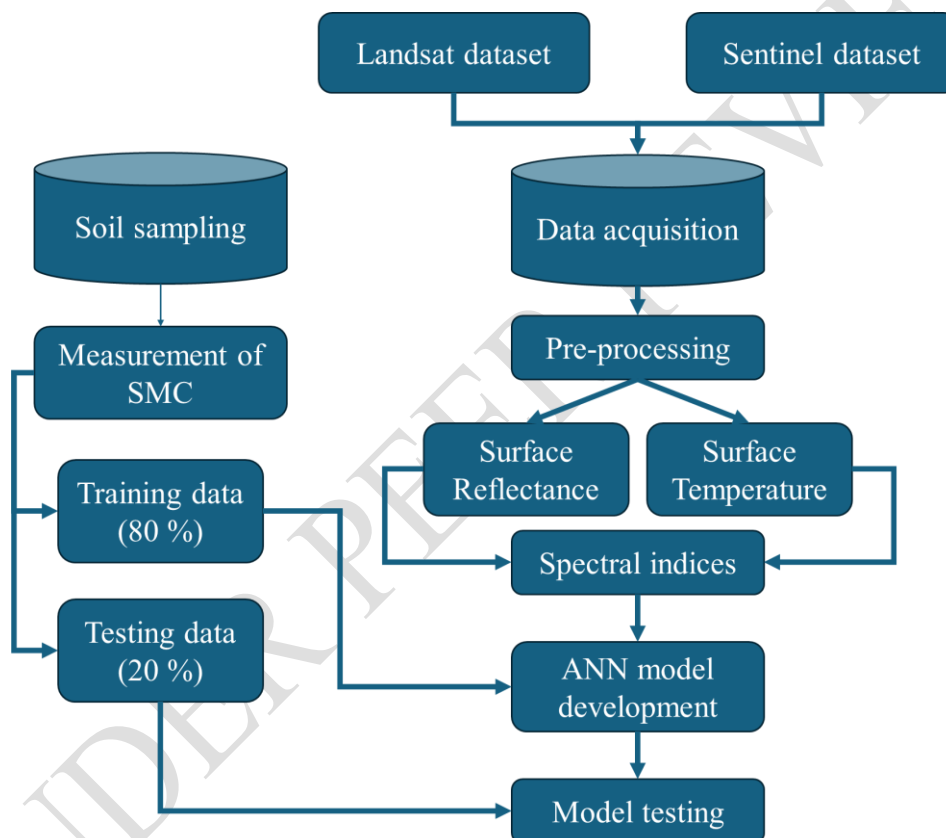


Fig.4: Flow diagram of the process

3. RESULTS & DISCUSSION

3.1 Measurement of soil moisture content

The soil moisture content (SMC) of soil samples was determined using gravimetric method (Reynolds, 1970). Overall, it was varied ranging from 3.40 % to 12.50 % with a mean value of 8.42 % and standard deviation of 1.62 %. The lowest and highest value of 3.40 % to 12.50 % were recorded in soil samples collected from Dwarka and Kalyanpur talukas, respectively (Table 2).

Table 2: Taluka wise range of soil moisture content

SMC (%) Taluka	Minimum	Maximum	Mean	Standard Deviation
Khambhalia	4.40	11.64	8.76	1.30
Kalyanpur	3.46	12.50	8.72	1.42
Dwarka	3.40	10.26	7.43	1.94

In total, 174 samples were recorded. From the recorded samples, map of soil moisture content over the study area was prepared using ArcMap. The map displayed in Fig. 5 will help in visualising SMC over the study area.

Values of soil moisture content were on lower side. This can be attributed to the timing of soil sampling was in second week of November month. During that time of the year, no crops are sown in the study area. Furthermore, Devbhumi Dwarka district has about two third area which is only rain fed (ACP: Devbhumi Dwarka, 2020); and lower cropping intensity leading to almost no sowing during sampling time. Spectral indices calculated are based on topsoil reflectance (Asfaw *et al.*, 2018; Gorji *et al.*, 2020; Li *et al.*, 2022), for this reason, soil sampling was also done in topsoil which tends be drier. The wastelands and majority parts of Dwarka taluka were having sandy loam soil which has lower water holding capacity (Kern, 1995). Certain similar studies done in BSh climates have also shown lower soil soil moisture content (Duff *et al.*, 1997; Chang *et al.*, 2016; Williams *et al.*, 2018; Meena *et al.*, 2020).

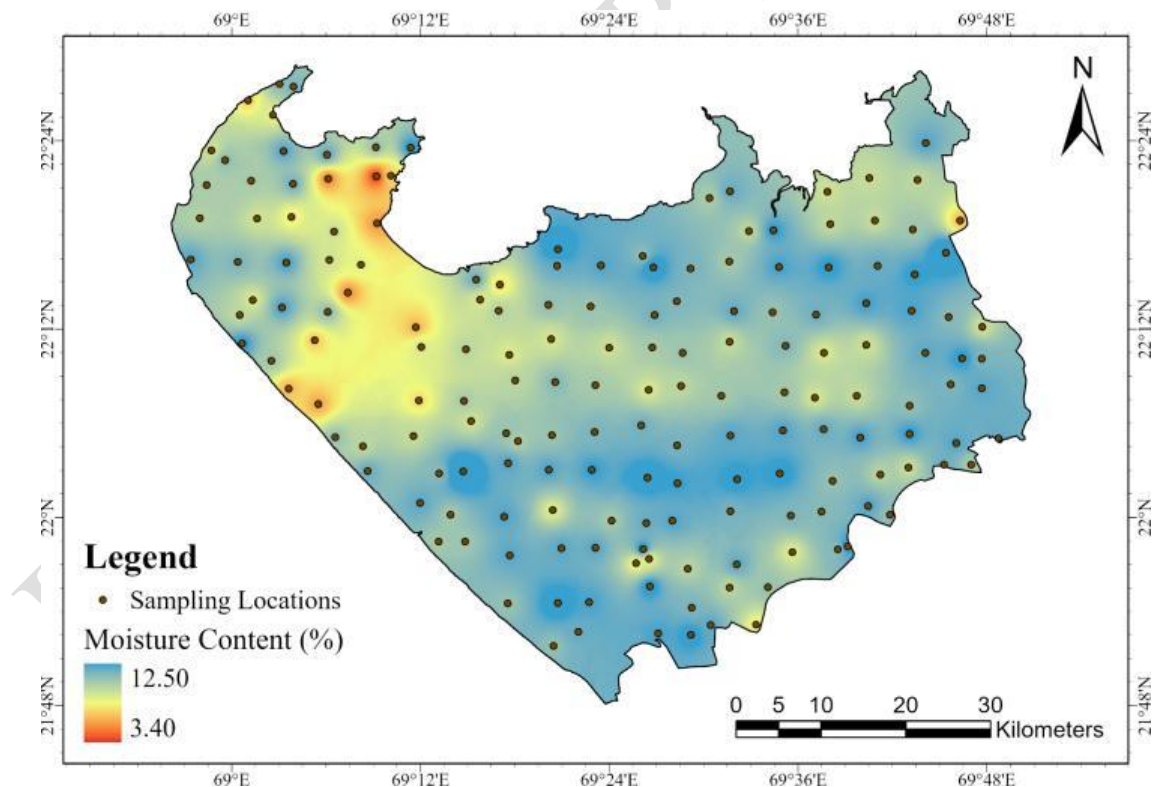


Fig. 5: Map of measured soil moisture content values at sampling locations

3.2 Spectral indices for soil moisture

All the maps of spectral indices are shown in Fig. 6 to Fig. 13. The performance of this individual indices with measured SMC is mentioned with coefficient of determination.

The Normalized Difference Water Index (NDWI) ranged from -0.61 to 0.58 for Landsat and -0.59 to 0.40 for Sentinel, with respective coefficients of determination (R^2) of 0.43 and 0.46. The Moisture Index (MI) varied between 0.17 to 2.11 (Landsat) and 0.32 to 1.78 (Sentinel), with R^2 values of 0.44 and 0.47. Normalized Difference Vegetation Index (NDVI) values were -0.34 to 0.59 (Landsat) and -0.28 to 0.46 (Sentinel), exhibiting R^2 values of 0.27 and 0.37. The Normalized Shortwave-Infrared Difference Soil Moisture Index (NSDSI3) had ranges of -0.20 to 0.71 (Landsat) and -0.04 to 0.46 (Sentinel), with R^2 values of 0.50 and 0.48. Land Surface Temperature (LST) for Landsat ranged from 20.92 °C to 31.18 °C, displaying a negative correlation (R^2 : 0.33). The Vegetation Supply Water Index (VSWI) for Landsat, normalized between 0 to 1, showed an R^2 value of 0.35. Notably, NSDSI3, MI, and NDWI exhibited high correlation with Soil Moisture Content (SMC), while NDVI, LST, and VSWI showed lower correlation, possibly due to limited vegetation in the study area.

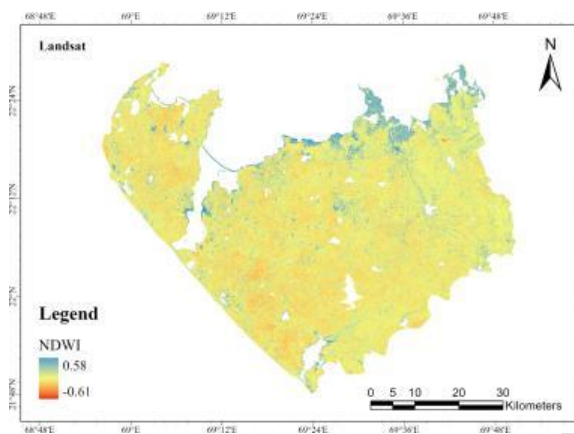


Fig. 6:NDWI map of study area using Landsat images

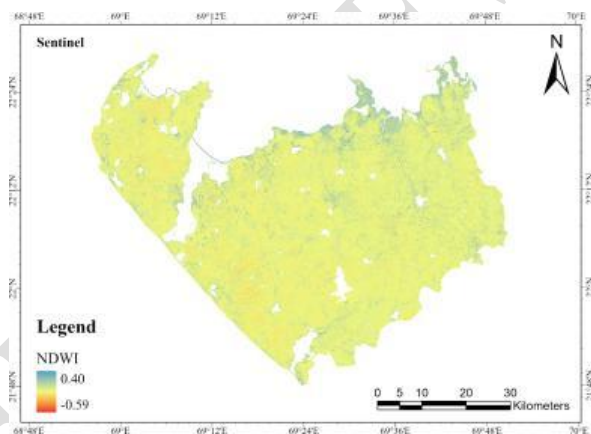


Fig. 7:NDWI map of study area using Sentinel images

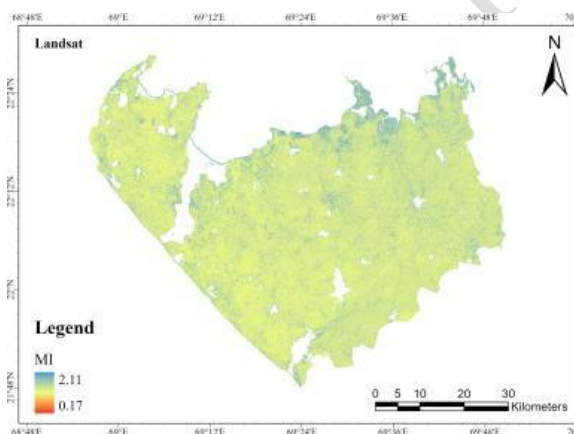


Fig. 8: MI map of study area using Landsat images

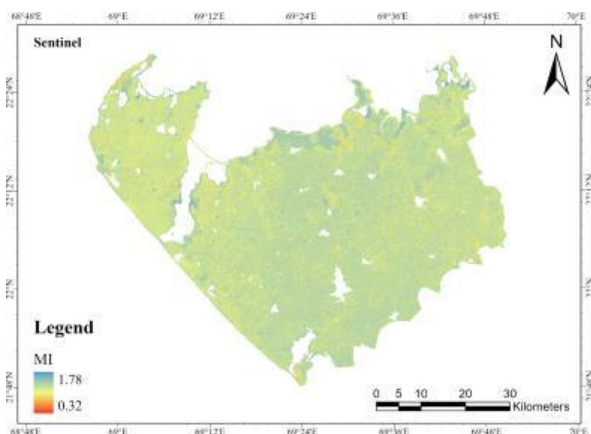


Fig. 9: MI map of study area using Sentinel images

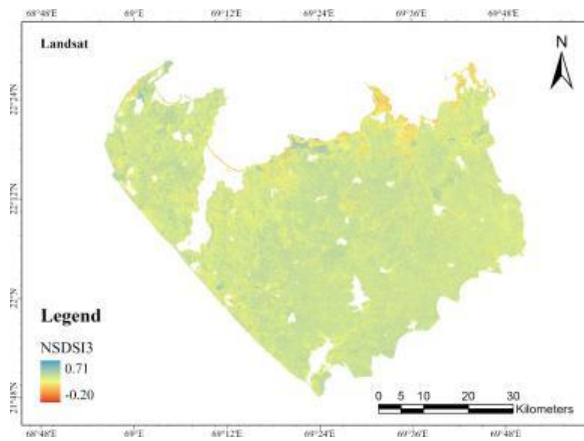


Fig. 10: NSDSI3 map of study area using Landsat images

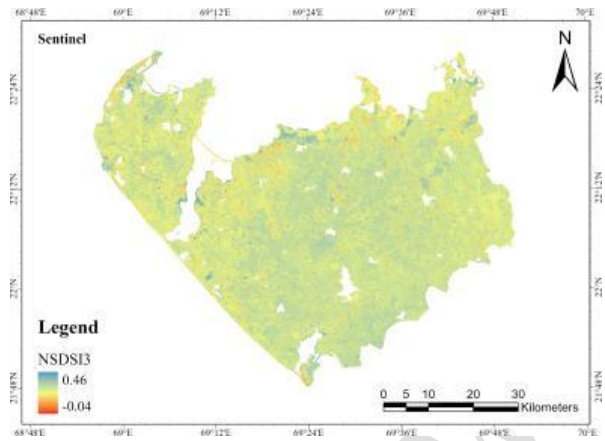


Fig. 11: NSDSI3 map of study area using Sentinel images

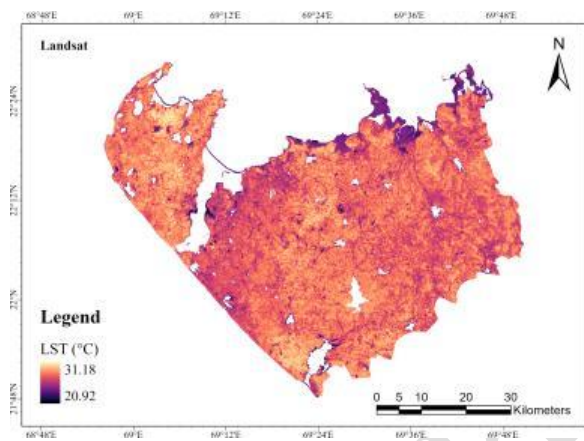


Fig. 12: LST map of study area using Landsat images

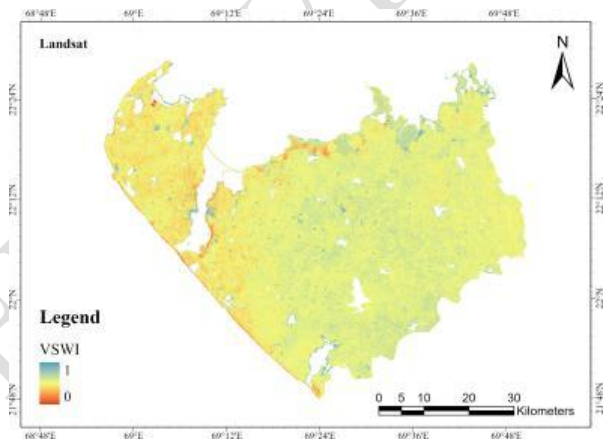


Fig. 13: VSWI map of study area using Landsat images

3.3 Modelling soil moisture content using ANN

The best input combination was selected based on the performance. Table 3 outlines the architecture of the three best-performing ANN models for both satellites. The performance of ANN models is shown in Table 4 and Table 5 for Landsat and Sentinel, respectively. While these models demonstrated good performance in training, their testing performance was not as robust, possibly due to a limited dataset for proper training. Among the models, ANN3L and ANN3S exhibited the highest performance indicators in both training and testing for Landsat and Sentinel data respectively, aligning with the findings of Hassan-Esfahani *et al.* (2015), suggesting that a larger number of inputs improved model performance. Similar observations were made by Chung *et al.* (2022) and Hachani *et al.* (2019) in estimating soil moisture in arid regions with limited input data. The results overall align well with studies in semi-arid to arid conditions with a lower number of input data. The performance of best performing model is visualized in Fig. 14 and Fig. 15 for Landsat and Sentinel, respectively.

Table 3: Best performing ANN models with Landsat and Sentinel data

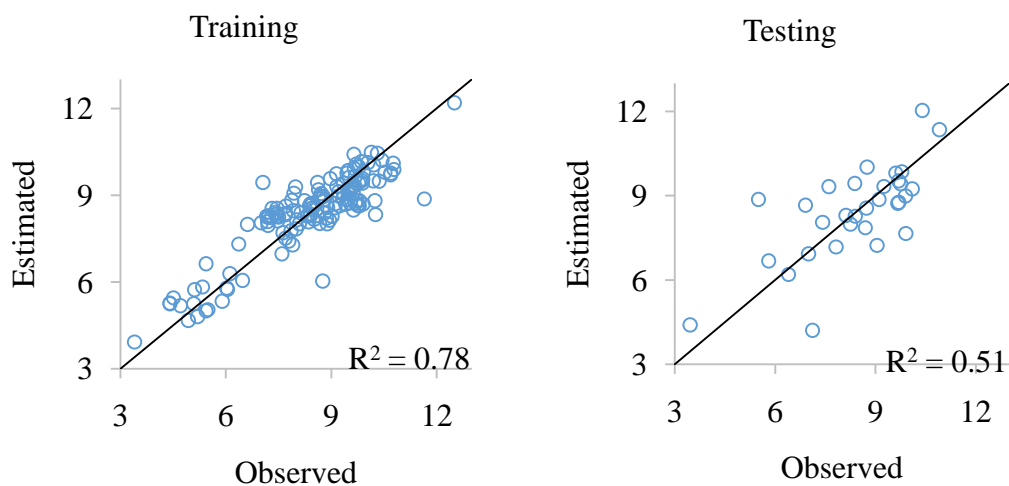
Model ID	Input variables	Architecture
Landsat		
ANN1L	LST, NDWI, MI, NSDSI3	4-12-1
ANN2L	NDVI, LST, NDWI, MI, VSWI, NSDSI3	6-17-1
ANN3L	NDVI, LST, NDWI, MI, VSWI, NSDSI3, B, G, NIR, R	10-15-1
Sentinel		
ANN1S	NDWI, MI, NSDSI3	3-12-1
ANN2S	NDWI, MI, NSDSI3, NDVI	4-10-1
ANN3S	NDVI, NDWI, MI, NSDSI3, B, G, NIR, R	8-14-1

Table 4: Performance of Landsat derived ANN models

Indicator	ANN1L		ANN2L		ANN3L	
	Training	Testing	Training	Testing	Training	Testing
RMSE (%)	0.64	1.75	0.81	1.47	0.76	1.23
R^2	0.84	0.14	0.75	0.31	0.78	0.51
NRMSE	0.08	0.21	0.10	0.17	0.09	0.15

Table 5: Performance of Sentinel derived ANN models

Indicator	ANN1S		ANN2S		ANN3S	
	Training	Testing	Training	Testing	Training	Testing
RMSE (%)	0.97	1.23	0.98	1.25	0.85	1.11
R^2	0.67	0.44	0.70	0.48	0.73	0.54
NRMSE	0.12	0.15	0.12	0.15	0.10	0.13

**Fig. 14: Comparison of observed vs estimated SMC (%) for ANN3L with Landsat data**

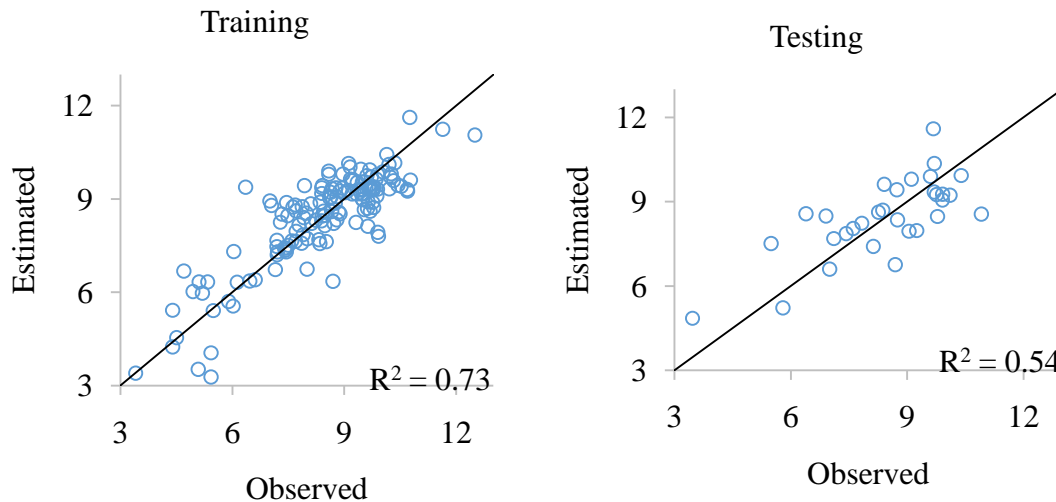


Fig. 15: Comparison of observed vs estimated SMC (%) for ANN3S with Sentinel data

4. CONCLUSION

The spectral indices, including NDVI, NDWI, MI, NSDSI3, LST, and VSWI, exhibited varied performance in capturing SMC. Notably, NSDSI3, MI, and NDWI demonstrate higher correlation with SMC, indicating their potential for accurate soil moisture estimation. However, NDVI, LST, and VSWI show lower correlation, possibly due to limited vegetation cover in the study area. The application of Artificial Neural Network (ANN) models for SMC prediction reveals promising results. Among the three best-performing ANN models for both Landsat and Sentinel data, ANN3L and ANN3S exhibit the highest performance indicators in both training and testing phases. The architecture of these models involves multiple input variables, emphasizing the significance of a diverse set of inputs for improved model performance. The observed limitations in testing performance may be attributed to the limited dataset for proper training, highlighting the need for further data collection to enhance model robustness.

In conclusion, the study provides valuable insights into soil moisture dynamics in the Devbhumi Dwarka region, emphasizing the influence of specific spectral indices on accurate estimation. The integration of ANN models enhances the predictive capability, with considerations for expanding the dataset to ensure more robust model performance in testing phases. These findings contribute to the broader understanding of soil moisture modelling in semi-arid climates, paving the way for refined agricultural management practices in the region. The developed ANN model will be useful in estimating soil moisture content in the semi-arid region of Devbhumi Dwarka.

5. REFERENCES

- ACP: Devbhumi Dwarka. 2020. Agriculture Contingency Plan for District: Devbhumi Dwarka. Available at [http://jau.in/ attachments/ AgriConti/](http://jau.in/attachments/AgriConti/) accessed 21 Jun. 2023.
- Alexakis, D. D.; Mexis, F. D. K.; Vozinaki, A. E. K.; Daliakopoulos, I. N. and Tsanis, I. K. 2017. Soil moisture content estimation based on Sentinel-1 and auxiliary earth observation products. *A hydrological approach. Sensors*. **17(6)**: 1455.

- Anonymous. 2022b. Khambhaliya Weather & Climate | Temperature & Weather By Month - Climate-Data.org. Available at <https://en.climate-data.org/asia/india/gujarat/khambhaliya-24445/> accessed 1 Nov. 2022.
- Asfaw, E.; Suryabhagavan, K. V. and Argaw, M. 2018. Soil salinity modeling and mapping using remote sensing and GIS: The case of Wonji sugar cane irrigation farm, Ethiopia. *Journal of the Saudi Society of Agricultural Sciences*. **17(3)**: 250-258.
- Carlson, T.N.; Gillies, R. R. and Schmugge, T. J. 1995. An interpretation of methodologies for indirect measurement of soil water content. *Agricultural and forest Meteorology*. **77(3-4)**: 191-205.
- Chang, C. T.; Sperlich, D.; Sabate, S.; Sanchez-Costa, E.; Cotillas, M.; Espelta, J. M. and Gracia, C. 2016. Mitigating the stress of drought on soil respiration by selective thinning: Contrasting effects of drought on soil respiration of two oak species in a Mediterranean forest. *Forests*. **7(11)**: 263.
- Chung, J.; Lee, Y.; Kim, J.; Jung, C. and Kim, S. (2022). Soil moisture content estimation based on Sentinel-1 SAR imagery using an artificial neural network and hydrological components. *Remote Sensing*. **14(3)**: 465.
- Dubayah, R.; Wood, E. F. and Lavallee, D. 2023. Multiscaling analysis in distributed modeling and remote sensing: an application using soil moisture. *In: Scale in remote sensing and GIS*, Routledge. pp. 93-112.
- Duff, G. A.; Myers, B. A.; Williams, R. J.; Eamus, D.; O'Grady, A. and Fordyce, I. R. 1997. Seasonal patterns in soil moisture, vapour pressure deficit, tree canopy cover and pre-dawn water potential in a northern Australian savanna. *Australian Journal of Botany*. **45(2)**: 211-224.
- EOS Data Analytics 2022. NDMI: Vegetation Index Equation And Values Interpretation. EOS Data Analytics. Available at <https://eos.com/make-an-analysis/ndmi/> accessed 17 June, 2023.
- Gao, B. C. 1996. NDWI-A normalized difference water index for remote sensing of vegetation liquid water from space. *Remote Sensing of Environment*. **58(3)**: 257-266.
- Garg, A.; Munoth, P. and Goyal, R. 2016. Application of soil moisture sensor in agriculture. *In: Proceedings of International Conference on Hydraulics, Water Resources and Coastal Engineering (Hydro2016)*, CWPRS Pune, India, December 8-10, 2016. pp. 8-10.
- Gojiya, K. M., Rank, H. D., Chauhan, P. M., Patel, D. V., Satasiya, R. M., & Prajapati, G. V. (2023). Remote Sensing and GIS Applications in Soil Salinity Analysis: A Comprehensive Review. *International Journal of Environment and Climate Change*. **13(11)**: 2149-2161.
- Gojiya, K. M., Rank, H. D., Chauhan, P. M., Patel, D. V., Satasiya, R. M., & Prajapati, G. V. (2023). Advances in soil moisture estimation through remote sensing and GIS: a review. *International Research Journal of Modernization in Engineering Technology and Science*. **5(10)**: 2669-2678.
- Gorji, T.; Yildirim, A.; Hamzehpour, N.; Tanik, A. and Sertel, E. 2020. Soil salinity analysis of Urmia Lake Basin using Landsat-8 OLI and Sentinel-2A based spectral indices and electrical conductivity measurements. *Ecological Indicators*. **112**: 106-173.

- GSDMA. 2022. Gujarat State Disaster Management Authority. Available at <http://gsdma.org/> accessed 17 September, 2022.
- Hachani, A.; Ouessar, M.; Paloscia, S.; Santi, E. and Pettinato, S. 2019. Soil moisture retrieval from Sentinel-1 acquisitions in an arid environment in Tunisia: Application of Artificial Neural Networks techniques. *International Journal of Remote Sensing*. **40(24)**: 9159-9180.
- Hassan-Esfahani, L.; Torres-Rua, A.; Jensen, A. and McKee, M. 2015. Assessment of surface soil moisture using high-resolution multi-spectral imagery and artificial neural networks. *Remote Sensing*. **7(3)**: 2627-2646.
- Kern, J. S. 1995. Geographic patterns of soil water- holding capacity in the contiguous United States. *Soil Science Society of America Journal*. **59(4)**: 1126-1133.
- Khanmohammadi, F., Homaei, M. and Noroozi, A. A. 2015. Soil moisture estimating with NDVI and land surface temperature and normalized moisture index using MODIS images. *Journal of Water and Soil Resources Conservation*, **4(2)**: 37-45.
- Li, X.; Li, Y.; Wang, B.; Sun, Y.; Cui, G. and Liang, Z. 2022. Analysis of spatial-temporal variation of the saline-sodic soil in the west of Jilin Province from 1989 to 2019 and influencing factors. *Catena*. **217**: 106-492.
- Liu, Y.; Qian, J. and Yue, H. 2021. Comprehensive evaluation of Sentinel-2 red edge and shortwave-infrared bands to estimate soil moisture. *IEEE Journal of Selected Topics in Applied Earth Observations and Remote Sensing*. **14**: 7448-7465.
- Meena, A.; Hanief, M.; Dinakaran, J. and Rao, K. S. 2020. Soil moisture controls the spatio-temporal pattern of soil respiration under different land use systems in a semi-arid ecosystem of Delhi, India. *Ecological processes*. **9(1)**: 1-13.
- Rabiei, S.; Jalilvand, E. and Tajrishy, M. 2021. A Method to Estimate Surface Soil Moisture and Map the Irrigated Cropland Area Using Sentinel-1 and Sentinel-2 Data. *Sustainability*. **13(20)**. 11355.
- Reynolds, S. G. 1970. The gravimetric method of soil moisture determination Part IA study of equipment, and methodological problems. *Journal of Hydrology*. **11(3)**: 258-273.
- Rohde, W. G. and Olson Jr, C. E. 1970. Detecting tree moisture stress. *Photogrammetric Engineering*. **36(6)**: 561-600.
- Rouse, J. W. R. H.; Haas, J. A.; Scell, D. W. and Harlan. J. C. 1974. Monitoring the Vernal Advancement of Retrogradation of Natural Vegetation, In: NASA/GSFC, Type III, 1974. Remote Sensing Center, Texas A&M University, Texas. p.371.
- Sedaghat, A.; Shahrestani, M. S.; Noroozi, A. A.; Nosratabad, A. F. and Bayat, H. 2022. Developing pedotransfer functions using Sentinel-2 satellite spectral indices and Machine learning for estimating the surface soil moisture. *Journal of Hydrology*. **606**: 127-423.
- Sharma, M.; Bangotra, P.; Gautam, A. S. and Gautam, S. 2022. Sensitivity of normalized difference vegetation index (NDVI) to land surface temperature, soil moisture and precipitation over district Gautam Buddh Nagar, UP, India. *Stochastic Environmental Research and Risk Assessment*. **36(6)**: 1779-1789.
- Sharma, P. K.; Kumar, D.; Srivastava, H. S. and Patel, P. 2018. Assessment of different methods for soil moisture estimation: a review. *J. Remote Sens. GIS*. **9(1)**: 57-73.

- Wang, J.; Peng, J.; Li, H.; Yin, C.; Liu, W.; Wang, T. and Zhang, H. 2021. Soil salinity mapping using machine learning algorithms with the sentinel-2 MSI in Arid Areas, China. *Remote Sensing* **13**(2): 305.
- Welikhe, P.; Quansah, J. E.; Fall, S. and Elhenney, W. Mc. 2017. Estimation of Soil Moisture Percentage Using LANDSAT-based Moisture Stress Index. *J Remote Sensing & GIS*. **6**(200): 2.
- Williams, E.; Ahenkorah, I.; Baffoe, E.; Awotoye, T. F.; Ephraim, G. L. and Asebiah, D. C. 2018. Application of geoelectric resistivity to determine soil moisture distribution. *American Journal of Engineering Research*. **7**(5): 113-124.
- Yue, J.; Tian, J.; Tian, Q.; Xu, K. and Xu, N. 2019. Development of soil moisture indices from differences in water absorption between shortwave-infrared bands. *ISPRS Journal of Photogrammetry and Remote Sensing*. **154**: 216-230.